Journal of Energy Storage 26 (2019) 100992

Contents lists available at ScienceDirect

Journal of Energy Storage

journal homepage: www.elsevier.com/locate/est

Evaluating energy and greenhouse gas emission footprints of thermal energy storage systems for concentrated solar power applications

Spandan Thaker, Abayomi Olufemi Oni, Eskinder Gemechu, Amit Kumar*

Department of Mechanical Engineering, 10-203 Donadeo Innovation Centre for Engineering, University of Alberta, Edmonton, Alberta T6G 1H9, Canada

ARTICLE INFO

Keywords:
Latent heat storage
Life cycle assessment
Net energy ratio
Sensible heat storage
Thermal energy storage
Thermochemical storage

ABSTRACT

Greenhouse gas emissions from the power generation sector contribute significantly to climate change. The use of thermal energy storage systems can reduce the sector's impact depending on factors such as plant energy performance and environmental friendliness. In this study, an Excel-based model was developed to evaluate the greenhouse gas emissions and net energy ratio for thermal energy storage technologies used in concentrated solar power applications. Five thermal energy storage systems were considered: two-tank indirect sensible heat storage, two-tank direct sensible heat storage, one-tank direct sensible heat storage, latent heat storage, and thermochemical storage. To capture the uncertainties in the results for each type of storage, a Monte Carlo simulation was performed by varying key operational and model parameters. With uncertainty taken into consideration, it was determined that the mean greenhouse gas emission values for two-tank direct sensible heat storage and one-tank direct sensible heat storage are 15 gCO_2-eq/kWh and 11 gCO_2-eq/kWh, respectively. The two systems offer higher energy performances and lower emissions than the other storage systems and thus the potential to be implemented commercially for concentrated solar power applications.

1. Introduction

Efforts are being made globaly to reduce the uman-activity related climate change impacts while greenhouse gas (GHG) emissions continue to rise. It is estimated that global GHG emissions could increase from 49 gigatonnes of carbon dioxide equivalent ($GtCO_2$-eq) in 2010 to approximately 700 $GtCO_2$-eq by 2030 [1]. The electricity production sector is a major contributor, it is responsible for nearly 25% of global GHG emissions [1]. The power sector must have a transition from fossil-fuel based sources to more renewable alternatives in order to meet the GHG emission reduction targets. The use of cleaner and more efficient energy technologies such as concentrated solar power (CSP) are a way forward. The International Energy Agency (IEA) announced a plan in 2014 to reduce about 2.1 gigatonnes of carbon dioxide annually through the installation of CSP plants by 2050 [2]. This plan prompted the search for energy efficient ways to store heat in CSP plants. One of the factors in CSP technologies that affect their energy performance is the intermittency of solar energy (little energy is delivered during the night and on cloudy days); this can be overcome by implementing thermal energy storage (TES) systems. TES systems have the potential to store energy in the form of heat for long durations, allowing the CSP plant to operate even when solar energy is intermittent.

TES systems are categorized into sensible heat, latent heat, and thermochemical storage. Sensible heat storage uses molten salt, a heat transfer fluid that can retain heat with a small change in temperature loss of approximately −17.22 °C per day [3]. Latent heat storage technology can store heat using a phase change material (PCM). Heat is stored in the process when the PCM is changed from solid to liquid and released when the PCM is changed from liquid to solid [4]. Thermochemical storage uses a reversible chemical reaction to store and release heat energy. Latent heat storage and thermochemical storage are still in the research and development phase since obtaining energy-efficient and low GHG emission profile heat transfer fluid is very challenging.

Progress in TES system development is expected to change the way heat is stored in the power generation industry and provide an opportunity to reduce fossil fuel use. However, whether to use TES technology depends on several factors such as plant energy performance and environmental friendliness. These factors are crucial to the sustainability of different TES systems in the future energy market. A cradle-to-grave life cycle assessment (LCA) is an appropriate means of evaluating the energy and environmental performances of TES systems. GHG emissions and net energy ratios (NERs) are the metrics used to examine and compare environmental and energy profiles of TES systems. Such evaluations provide useful insights into life cycle stages of TES systems and enhance sustainable decision-making in power

* Corresponding author.
E-mail address: amit.kumar@ualberta.ca (A. Kumar).

https://doi.org/10.1016/j.est.2019.100992
Received 6 February 2019; Received in revised form 5 September 2019; Accepted 30 September 2019

Abbreviations

CSP	Concentrated solar power
CO_2	Carbon dioxide
GHG	Greenhouse gas
GJ	Gigajoule
Gt	Gigatonne
gCO_2-eq	Grams of carbon dioxide equivalent
IEA	International Energy Agency
kWh	Kilowatt hour
LCA	Life cycle assessment
NER	Net energy ratio
PCM	Phase change material
R&D	Research and development
SM	Solar multiple
S1	Indirect sensible heat storage using two tanks
S2	Direct sensible heat storage using two tanks
S3	Direct sensible heat storage using one tank
S4	Latent heat storage using one tank
S5	Thermochemical heat storage
TES	Thermal energy storage
Tkm	Ton-kilometer

Symbols

A	Total heat exchanger area
c_p	Specific heat capacity
h	Enthalpy
$\dot{m}$	Mass flow rate
N	Total life (years)
$\dot{Q}$	Rate of heat transfer
$\dot{Q}_{loss}$	Rate of heat loss
T	Temperature of heat transfer fluid
$\dot{W}$	Rate of work
ΔE_k	Change in kinetic energy
ΔE_p	Change in potential energy

generation. LCA has been applied for a comparative evaluation of various systems [5,6]. One of the critical aspects of a successful comparative LCA is the definition of system boundaries. Unclear or inappropriate boundary definitions between systems lead to unreasonable comparative studies and decision-making. Therefore, for a good selection of system boundaries, it is essential to examine the system from both the functional and technical perspectives.

There are some LCA studies on TES systems. Some focus on the life cycle environmental impacts of selected TES systems independent of the system energy performance and vice versa. Decisions are hard to make in many of these studies because of differences in goal and scope definition, system boundary selection, the choices of modeling parameters, and the level of uncertainty associated with those variations. Uncertainty is a key element in LCA, and it needs to be performed to better understand the results and interpret their implications. Earlier LCA studies on TES systems aimed to understand the environmental performance of individual storage system in terms of GHG emissions and NER. The GHG emission characterization of individual TES system, with different system boundaries, has been a subject of discussion in several papers [7,8], while other papers examine the energy performance of TES systems [9,10]. A study by Burkhardt et al. evaluated the life cycle environmental impacts of a hypothetical 103 MW parabolic trough, wet-cooled CSP plant with 6.3 h of thermal storage capability [11]. The study deduced that the type of cooling system and nitrate salt used as a storage medium influence the environmental impacts of the system. While a thorough LCA was conducted for a parabolic trough CSP plant, it would be difficult to compare the results with other TES systems due to the differences in the modeling parameters. Adeoye et al. conducted a comparative study to assess the environmental impact of using molten salt and concrete as the storage medium [12]. Although an extensive comparison was conducted, the study only considered sensible heat storage; other TES systems such as latent heat and thermochemical storage were not considered [12]. Some studies examine the environmental impacts of using hybrid systems. For example, Magrassi et al. developed a comparative LCA study to evaluate the environmental impact of a 100 kW photovoltaic plant and a 100 kW solar-hybrid gas turbine CSP plant [13]. Good et al. examined the performance of a hybrid solar, photovoltaic, and thermal systems used for a district heating application [14]. Lechon et al. evaluated the life cycle GHG emissions for a 17 MW central tower CSP plant and a 50 MW parabolic trough CSP plant integrated with a natural gas-fired auxiliary boiler [15]. Larrain and Escobar focused on the energy performance of a CSP plant with a hybrid direct steam generation plant using natural gas as the backup fuel [16]. A study by Burkhardt et al. performed an LCA for a parabolic trough CSP plant with a two-tank TES system and also considered other design alternatives for TES that could minimize GHG emissions and water consumption [5].

One of the main purposes of LCA is to compare the environmental performances of different products with the same functionality. Some researchers performed LCA to compare the environmental performance of two systems. For example, Oro et al. examined the GHG emissions for sensible and latent heat storage systems while not considering thermochemical storage [8]. Other limitations identified from the study by Oro et al. are the differences in the assumptions and modeling parameters. For example, the study did not consider the heat transfer fluid circulating in the TES system and assumed the total plant life to be 20 years. To the best of the authors' knowledge, there is no comprehensive comparative life cycle GHG emissions assessment of sensible heat, latent heat, and thermochemical storage.

The results from these earlier studies cannot be directly compared because of differences in system boundaries and the lack of information on the reliability of model uncertainties. Further research is required to address the limitations associated with decision-making in TES systems and to examine model uncertainties for TES technologies. With the aim of filling the literature gap, this study, therefore, aims to develop a bottom-up data-intensive LCA model to determine the GHG emissions and NER for sensible heat, latent heat, and thermochemical storage. It is the first comprehensive LCA study that considers all types of TES technologies. The general objective is accomplished through the following specific objectives:

1. The goal and scope of the study is set to have a common system boundary for sensible heat, latent heat, and thermochemical storage technologies.
2. Life cycle inventory data is developed to assess the GHG emissions and NERs for the TES technologies.
3. Sensitivity and uncertainty analyses are performed to assess the impact of different parameters on the GHG emissions and NERs for each storage technology for better decision-making.

2. Methods

The LCA method presented in this research is in accordance with International Organization for Standardization (ISO) 14040 and 14044 [17,18]. The ISO provides a guideline principle and framework on how to conduct LCA. LCA has four major phases: goal and scope definition, inventory analysis, life cycle impact assessment, and interpretation [19]. This section discusses each aspect of the LCA stages in the context of the study.

2.1. Goal and scope definition

The goal of the research is to perform a bottom-up process specific comparative LCA of sensible heat, latent heat, and thermochemical storage systems with the aim of identifying the most environmentally sustainable alternative system. An Excel-based model was developed to evaluate the GHG emissions and NER for each TES system.

As stated earlier, there are LCA studies on different TES systems; however, each study uses different system boundary definitions, input and output requirements, operational conditions, parameters, and so on. Any comparative assessment using only the existing literature is subject to high level of uncertainty. To address this problem, the study attempts to provide comprehensive LCAs of TES systems by defining the same boundaries and input parameters for each.

The functional unit is one of the key elements in an LCA study, especially when comparing the environmental performance of several products. This unit provides a reference through which the input and output requirements from different systems are normalized. Here the functional unit is defined as one kWh of energy delivered from stored heat.

Fig. 1 shows the common system boundary that was established to accurately assess and compare the GHG emissions and NERs of different TES systems. The following life cycle stages were included for each system: material extraction and production, construction, transportation, operation, dismantling, and disposal. Material and energy requirements at each stage were computed for the individual component used in the TES systems (i.e., material used in the construction of the heat exchangers, piping, storage tanks, and pumps). Subsequently, GHG emission factors (gCO_2.eq/kWh) and energy consumed in producing these materials were determined through the Greenhouse Gases, Regulated Emissions, and Energy Use in Transportation (GREET) model [20]. Electricity consumption emissions in the production phase were also considered. For the NER evaluation, the energy consumption in each unit operation during individual life cycle phase was calculated. The NER for each scenario was evaluated using mass and energy balances for individual equipment including the storage tanks, heat exchangers, and pumps. The mass and energy balances were used to compute the heat lost from storage tanks and heat exchangers. The heat gained in the pumps was also computed. The net heat delivered in each scenario was evaluated to compare the energy yield of individual TES technologies.

2.2. Process description

The following alternative TES systems were considered: two-tank indirect sensible heat storage (S1), two-tank direct sensible heat storage (S2), one-tank direct sensible heat storage (S3), latent heat storage (S4), and thermochemical storage (S5). This section briefly describes the main processes for each TES systems, which are illustrated in Figs. 2–6. Detailed descriptions and schematics of each process can be found in the authors' previous publication [21].

Two-tank indirect sensible heat storage (S1): As shown in Fig. 2, Dowtherm A©/Therminol VP© fluid is used to transfer heat to water and produce superheated steam in a heat exchanger (HX 2). This operation takes place during the daytime when ample sunlight is available and during peak demand. During low energy demand, excess heat from the sun is stored in the molten salt and can be extracted during the night in the heat exchanger (HX 1). The operating temperature in S1 ranges from 320–400 °C [22]. A heat-tracing system (heating cables) is required to prevent the Dowtherm A©/Therminol VP© fluid and the molten salt from freezing. High performance mineral-insulated heating cables are considered for this application as they offer high temperature maintenance, high temperature exposure, and high watt density. The heating cables use electrical energy to pre-heat the pipeline and storage tanks. The same concept is applied for two-tank direct sensible heat storage, one-tank direct sensible heat storage, and latent heat storage systems.

Two-tank direct sensible heat storage (S2): This scenario (shown in Fig. 3) uses molten salt as the heat transfer medium to convert water into superheated steam in the heat exchanger. Thus, it does not require an additional heat exchanger and pump. Instead, the system uses a central tower CSP plant configuration to reflect sunlight, which heats molten salt to operating temperatures of approximately 290–565 °C [22]. S2 has a higher operating temperature range and potentially higher energy yield than S1.

One-tank direct sensible heat storage (S3): This scenario, shown in Fig. 4, operates on the same principle as S2. The key difference is the reduced tank volume and molten salt requirement, which could reduce the material needed for plant construction.

Latent heat storage (S4): This scenario, shown in Fig. 5, uses encapsulated PCM pellets that remain in the storage medium without being mixed with molten salt. The PCM in the top of the tank absorbs part of the heat from the hot molten salt and is melted. The melted PCM then settles to the bottom of the tank while the pellets at the bottom float to the top. Here, both PCM and molten salt are considered as heat transfer mediums. However, molten salt is the working fluid as it is pumped for circulation through the system. The heat retained from melted PCM is released into the cold molten salt that enters the tank bottom. Then the PCM pre-heats the cold molten salt leaving the tank before being further heated in the solar field.

Thermochemical heat storage (S5): The input ammonia stream is heated in the solar field by concentrating heat onto a central tower using mirrors (Fig. 6). The heated ammonia enters at around 950 °C and 20 MPa. Ammonia is dissociated to a hydrogen and nitrogen gas mixture in the presence of a catalyst inside the dissociation reactor. The mixture is then cooled to ambient temperature in a heat exchanger (HX

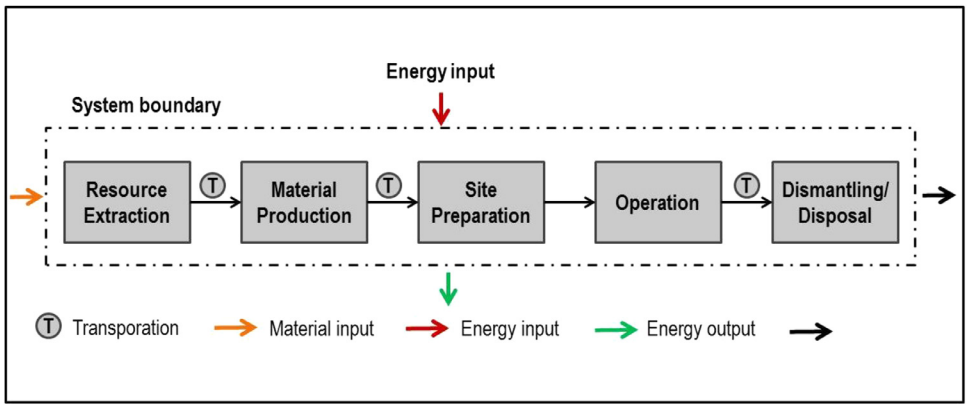

Fig. 1. Common system boundary for thermal energy storage systems.

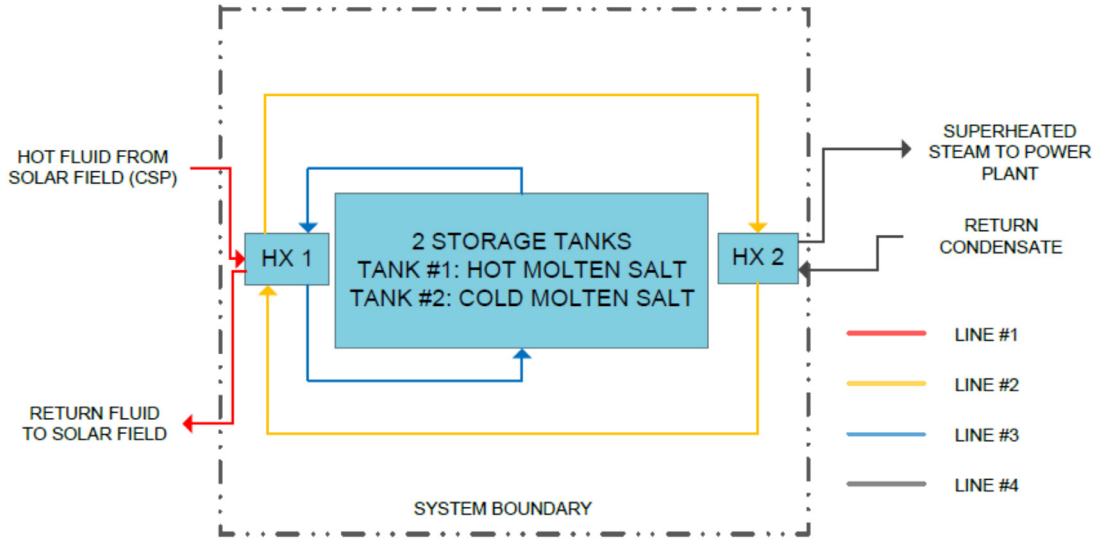

Fig. 2. Two-tank indirect sensible heat storage system (S1) (derived from [21]).

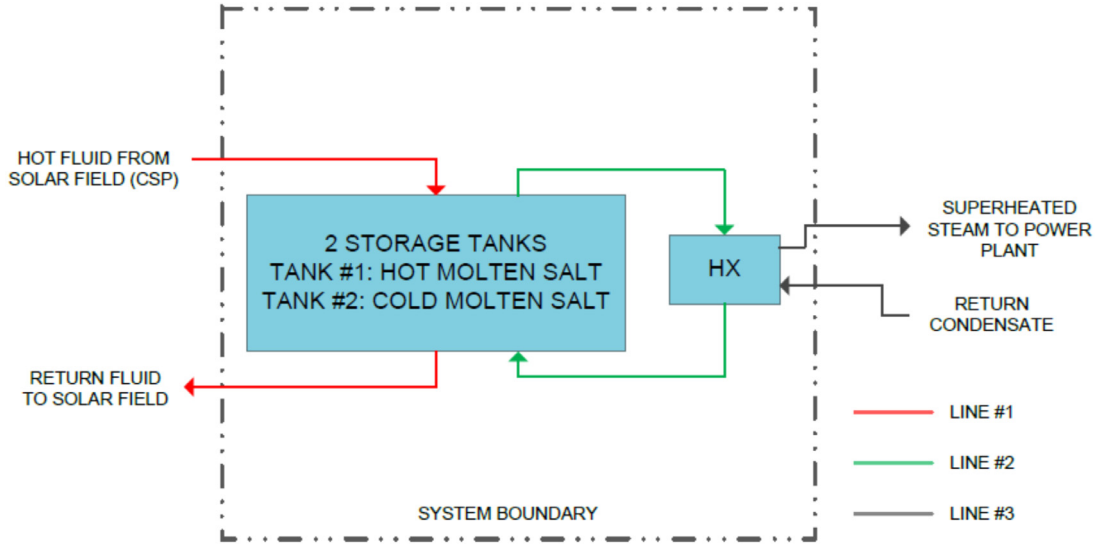

Fig. 3. Two-tank direct sensible heat storage system (S2) (derived from [21]).

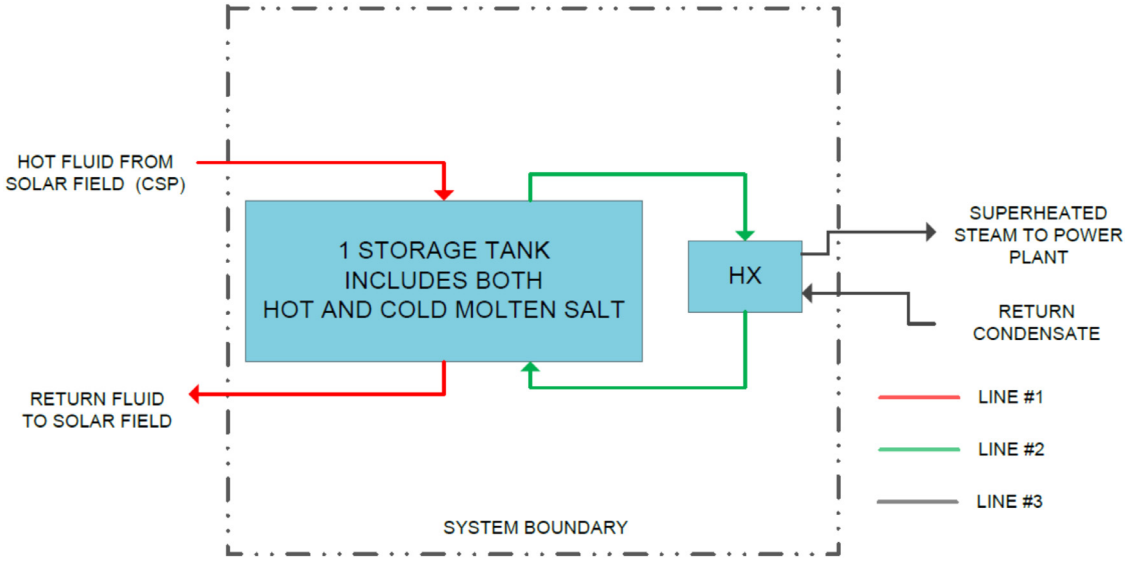

Fig. 4. One-tank direct sensible heat storage system (S3) (derived from [21]).

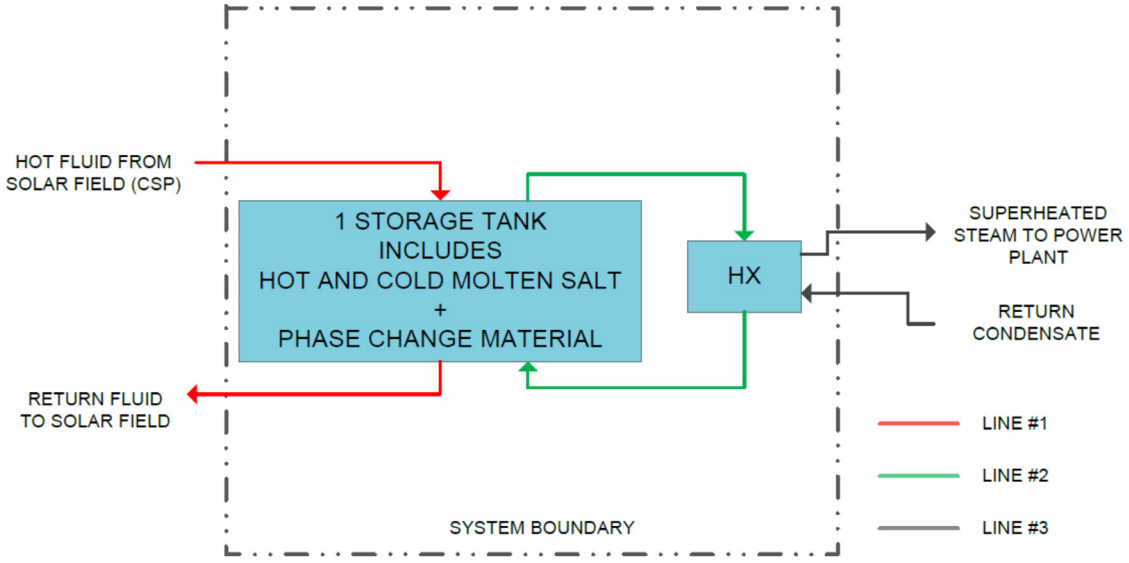

Fig. 5. Latent heat storage system (S4) (derived from [21]).

1) before being stored in a two-phase high-pressure storage tank with minimal heat loss [23]. To recover stored heat, the hydrogen and nitrogen gas mixture is preheated in a heat exchanger (HX 2) to approximately 275 °C. The gas mixture is then diverted to a synthesis reactor to produce ammonia. The synthesis reaction releases large amounts of heat that is used in another heat exchanger (HX 3) to convert water to superheated steam at approximately 430 °C and 10 MPa [24]. The high-pressure superheated steam can be used in applications such as power generation and process heating.

2.3. Life cycle inventory calculation

Material and energy inputs along with associated GHG emissions for each life cycle stage (resource extraction, material production, site preparation, operations, transportation, and dismantling) are considered. The material requirement for TES components (the storage tank, piping, pumps, heat exchangers, heat-tracing system [heating cables], molten salt, and synthetic oils [Dowtherm A©/Therminol VP©]) were computed using mass and energy balances. Data from GREET was used to compute the emissions and energy input requirement for the materials production phase [20]. Key input resources such as molten salt (sodium nitrate and potassium nitrate [25]), Dowtherm A©/Therminol VP© [26], and phase change materials (lithium carbonate [27] and potassium carbonate [5]) are assumed to be manufactured separately in different locations. Since a case study for Alberta is the focus of this work, the emission factors and energy requirement to transport material from their respective manufacturing sites to the plant (Medicine Hat, Alberta) are taken to be 202 gCO_{2eq}/tkm and 1148 kJ/tkm, respectively [28]. However, the method and the parameters considered in this study would be valid for other locations with minor adjustments in the model. Emissions from site preparation in the construction of the plant and downstream emissions at the end-of-life stages (dismantiling and disposal) were also considered. The emission factors corresponding to the electricity consumed during the production phase were obtained from the literature. The emissions from the operations phase were due to electricity consumption in pumps. The life cycle GHG emission factor for using solar photovoltaic energy as the source of electricity in the operational phase was considered to be 41 gCO_{2-eq}/kWh [29]. For the end-of- life cycle stage, only the transportation effort to dispose Dowtherm A©/Therminol VP© at the

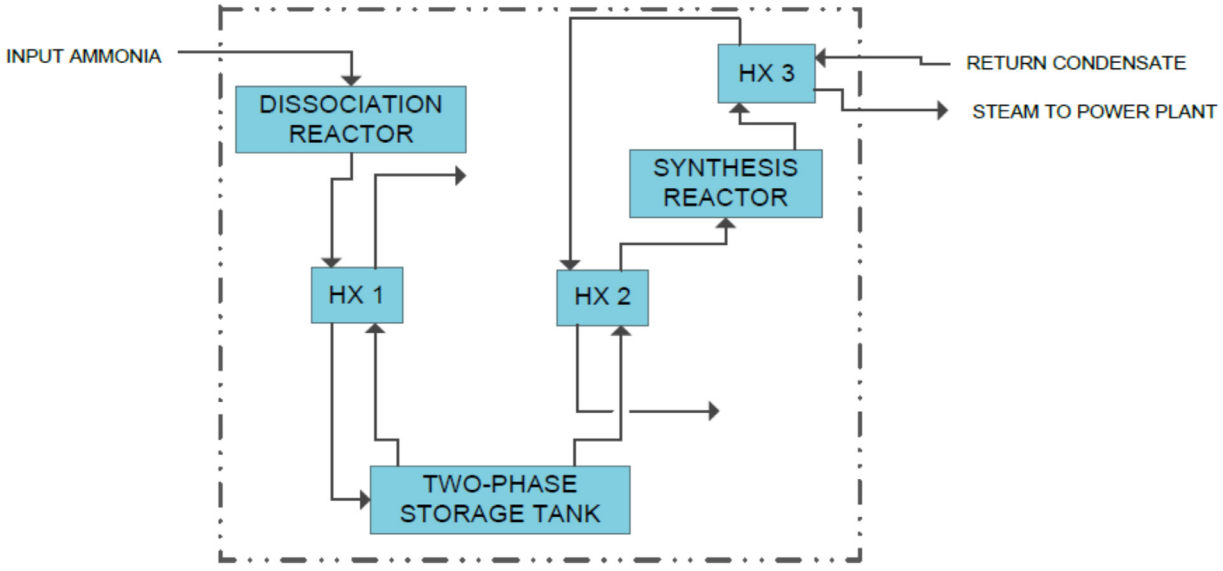

Fig. 6. Thermochemical heat storage (S5) (derived from [21]).

incineration facility in Whitecourt, Alberta was considered [30]. Other end-of-life cycle treatments such as recycling, landfilling, and incineration are beyond the scope of the study.

The design consideration and the material and energy requirement calculation for each unit operation are presented below.

Pressure vessels: The thickness of a pressure vessel determines how much material is required to construct the vessel. Pressure vessels are designed based on the internal pressure and maximum allowable stress of the material. According to the ASME Boiler and Pressure Vessel Section VIII standard, the minimum wall thickness of a pressure vessel with known variables such as design pressure (P), vessel outer radius (R), maximum allowable stress (S), and joint efficiency (E) can be calculated as shown in Eq. (1) [31]. If the thickness is less than one half of the inner radius, then the minimum thickness shall be the greater thickness of the values corresponding to circumferential stress and longitudinal stress. The minimum thickness computed in Eq. (1) corresponds to the greater thickness.

$$t = \frac{P*R}{(S*E) + (0.4*P)} \tag{1}$$

The allowable stress in Eq. (1) is a function of the operating temperature. The allowable stress for carbon steel is assumed to be 103 MPa for operating temperatures up to 300 °C [32]. The allowable stress for stainless steel is taken to be 65.4 MPa and 103 MPa for operating temperatures up to 600 °C and 450 °C, respectively. The operating pressure in the ammonia reactors and storage tank is considered to be around 20 MPa [23], and the vessel outer diameter and vessel height are assumed to be 4.9 m and 7.2 m, respectively.

Storage tank: The wall thickness of a molten salt storage tank is computed using the American Petroleum Institute (API) 650 standard for storage tanks [33] (Eq. (2)):

$$t = \frac{2.6*D*(H-1)*G}{S} + \mathrm{CA} \tag{2}$$

where, t, D, H, G, S, and CA are tank wall thickness (in), nominal tank diameter (ft), tank height (ft), specific gravity of fluid in the tank, maximum allowable stress (psi), and corrosion allowance (in), respectively [33]. The mass of the tank is evaluated by multiplying the tank volume (computed by multiplying wall thickness and tank surface area) with its material density.

Process piping and heat exchanger tubes: The wall thickness was computed using both the *Pipeline Rules of Thumb Handbook* [34] and the ASME B31.3 standard for process piping [35] and was calculated using Eq. (3). Since the pipe wall thickness is one sixth of the outer diameter, the following equation can be used to compute the wall thickness of a straight pipe under internal pressure:

$$t = \frac{P*D_i}{(2*S*E) + (2*P*(Y-1))} \tag{3}$$

where t, P, D_i, S, E, Y correspond to the pipe wall thickness (m), internal pressure (Pa), inner pipe diameter (m), maximum allowable stress (Pa), joint efficiency, and temperature coefficient, respectively. The mass of the pipes is computed using the same procedure as for the storage tank. Table 1 summarizes the main material requirement results for different unit operations. The values correspond to 50 MW for S1 and 100 MW for S2–S5.

Heat-tracing system: high-performance mineral-insulated heating cables are manufactured using a solid alloy or copper conductor, compacted magnesium oxide insulation, and seamless alloy 825. The cable has a maximum maintenance temperature of 500 °C, minimum installation temperature of −60 °C, and maximum watt density of 262 W per meter [38]. The dimension of the pipeline and its heat loss, the dimension of the tank, and the watt density were used to calculate the total operational energy requirement and associated GHG emissions. The emissions associated with the material extraction and cable manufacturing stages are outside the scope of this study since there is limited information on them; however, their impact is assumed to be minimal.

2.4. Greenhouse gas emissions and net energy ratio evaluation

The Intergovernmental Panel on Climate Change's 100-year global warming potential was used to translate the inventory results into GHG emissions as a CO_2-eq per the functional unit (1 kWh).

NER is defined as the ratio of net heat delivered by the thermal storage system, measured in gigajoules (GJ), to the fossil fuel input to the thermal storage system (GJ), as shown in Eq. (4):

$$\mathrm{NER} = \frac{Q_{\mathrm{delivered}}}{\sum \text{Energy use in life cycle phases}} \tag{4}$$

The NER is a unitless metric evaluated as the ratio of the heat output from thermal storage to the fossil fuel input. from individual life cycle phase (i.e., production, construction, transportation, operation, dismantling, and disposal). The NER examined in this study focuses solely on the thermal storage components. The heat losses incurred in the solar field and power plant components are not considered. The net heat delivered by the TES system ($Q_{\mathrm{delivered}}$) is computed using Eq. (5).

$$Q_{\mathrm{delivered}} = \sum Q_{\text{gain in pumps}} - \sum Q_{\text{loss in heat exchanger and tanks}} \tag{5}$$

The heat gain in pumps is computed using Eqs. (6) and 7 [39]:

$$T_{\mathrm{rise}} = \frac{P_s*(1-\eta)}{c_p*V*\rho} \tag{6}$$

$$Q_{\text{gain in pumps}}\ (\mathrm{kJ}) = m*c_p*T_{\mathrm{rise}} \tag{7}$$

where P_s, η, c_p, V, ρ, m, represent brake power (kW), pump efficiency, specific heat capacity (kJ/kg K), volume flow rate (m^3/s), density (kg/m^3), and mass of fluid (kg), respectively.

The heat loss (GJ) from a heat exchanger depends on the efficiency

Table 1
Material requirement in metric tonnes (MT) [3,5,36,37].

	S1[a]	S2	S3	S4	S5
Aluminum	0.3	23	23	23	23
Concrete	4903	55,880	55,880	55,880	55,880
Copper	1	52	52	52	52
Iron	0.4	0.8	0.8	0.8	0.8
Polyethylene	4	2	2	2	2
Polypropylene	39	0.03	0.03	0.03	0.03
Heat transfer medium					
Molten salt	34,089	34,771	23,181	8693	N/A
Dowtherm A©/Therminol VP© HTF	37,199	N/A	N/A	N/A	N/A
PCM	N/A	N/A	N/A	26,078	N/A
Ammonia	N/A	N/A	N/A	N/A	25,360
Storage tanks/pressure vessel					
Carbon steel	2041	2041	N/A	N/A	N/A
Stainless steel	2107	2107	1405	738	1373
Mineral wool	284	337	169	169	24
Fiberglass	2.7	3.2	1.6	1.6	0.21
Foam glass	23	34	34	34	N/A
Firebrick	66	95	95	95	N/A
Heat exchangers					
Stainless steel	233	20	20	20	4
Piping					
Carbon steel	71	42	42	42	273
Stainless steel	197	627	627	627	658
Calcium silicate	319	158	158	158	164
Pumps					
Stainless steel	13	13	13	13	13
Total stainless steel	2549	2767	2064	1397	2047
Total carbon steel	2112	2083	42	42	273

[a] S1, two-tank indirect sensible heat storage; S2, two-tank direct sensible heat storage; S3, one-tank direct sensible heat storage; S4, latent heat storage; S5, thermochemical storage.

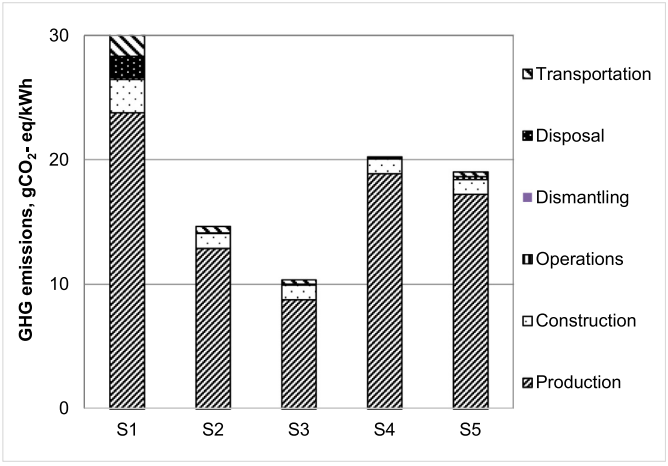

Fig. 7. Life cycle GHG emissions for thermal energy storage systems (S1: two-tank indirect sensible heat storage; S2: two-tank direct sensible heat storage; S3: one-tank direct sensible heat storage; S4: latent heat storage; S5: thermochemical storage).

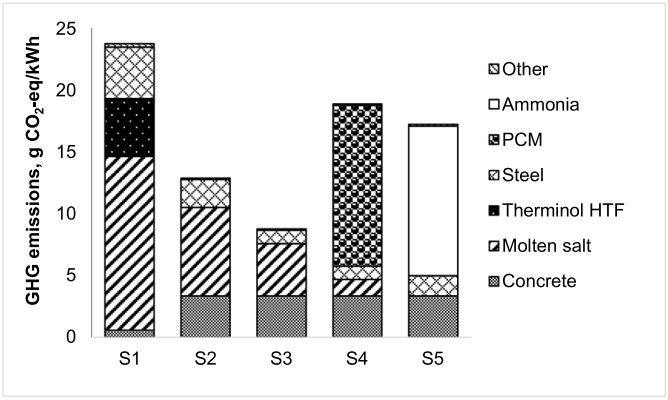

Fig. 8. Elemental contribution of GHG emissions from the production stage (S1: two-tank indirect sensible heat storage; S2: two-tank direct sensible heat storage; S3: one-tank direct sensible heat storage; S4: latent heat storage; S5: thermochemical storage).

(η) of the heat exchanger. The efficiency of the heat exchanger is considered to be 95% [40], as shown in the energy balance in Eq. (8). A wide range of heat exchanger efficiencies was considered to capture the uncertainty associated with heat exchangers.

$$\dot{Q} = \eta^*[\dot{m}_1 c_{p1}(T_2 - T_1)]_{\text{Fluid},1} = [\dot{m}_2 c_{p2}(t_2 - t_1)]_{\text{Fluid},2} \quad (8)$$

The heat loss from the molten salt storage tank can be computed using Eq. (9):

$$Q_{\text{tank}} = m_{\text{molten salt}}{}^* c_p{}^*(\Delta T) \quad (9)$$

where $m_{\text{molten salt}}$, c_p, and ΔT represent the molten salt mass, specific heat capacity of molten salt, and change in temperature loss over a period of one day, respectively. The change in temperature loss for molten salt is considered to be around $-17.22\,^{\circ}\text{C}$ per day [41].

3. Results and discussion

3.1 GHG emissions

The global GHG emissions of all the TES systems considered are shown in Fig. 7. With 11 gCO_2-eq/kWh, S3 shows the lowest GHG emissions, followed by S2. S1 has the highest GHG emissions. As the diagram shows, the largest share of GHG emissions in all TES systems is from production. This emissions share can influence overall results and is mainly due to fossil fuel and electricity consumption by the production facilities. Transportation and construction GHG emissions in S1 are considerably higher than in the other systems. The transportation GHG emissions are from delivering large quantities of Dowtherm A©/Therminol VP© from the manufacturing facilities to the plant site and the disposal site. Dowtherm A©/Therminol VP© HTF used in S1 degrades over its life cycle and must be disposed off at the end of the plant life. Since S2–S5 do not use Dowtherm A©/Therminol VP© as the heat transfer medium, the GHG emissions contribution from the transportation effort for these scenarios is very low.

The GHG emission variations in the different TES technologies can be attributed to their energy requirements at the production phase. Fig. 8 provides a detailed breakdown of GHG emissions during the production stage for each system. For example, the production of molten salt and Dowtherm A©/Therminol VP© in S1 shows the highest GHG emissions contribution compared to the other systems, around 80%. This is because S1 has a parabolic trough CSP plant configuration, which needs both Dowtherm A©/Therminol VP© and molten salt as the heat transfer medium. Though not so high, the significance of molten salt is reflected in the process GHG emissions of S2 and S3. S3 has the lowest production GHG emissions of all the systems because its tank volume requirement is approximately 66% that of a two-tank system [42,43]. S3 uses only one tank to store the molten salt and S2 uses two. Production GHG emissions in S4 come primarily from PCMs, as 75% of the tank's volume is PCMs and 25% is molten salt [42]. PCMs have high energy density and effectively store heat, thereby lowering the storage tank volume requirement by 65% [42]. In S5, the high

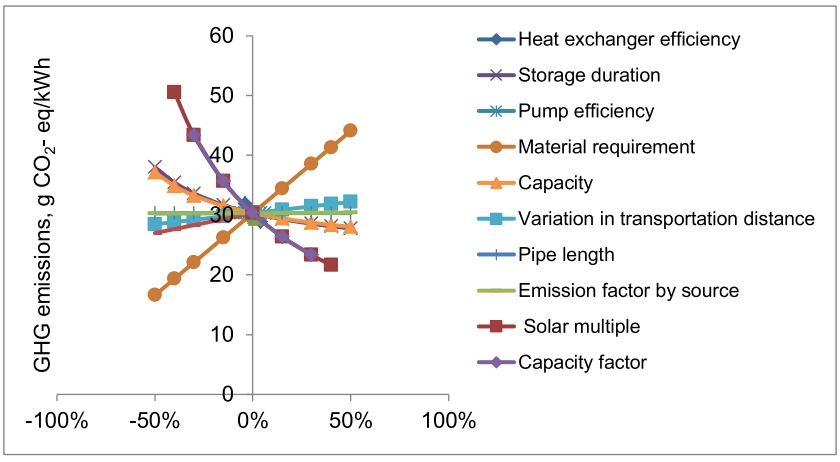

Fig. 9. GHG emissions sensitivity plot for 2-tank indirect sensible heat storage (S1).

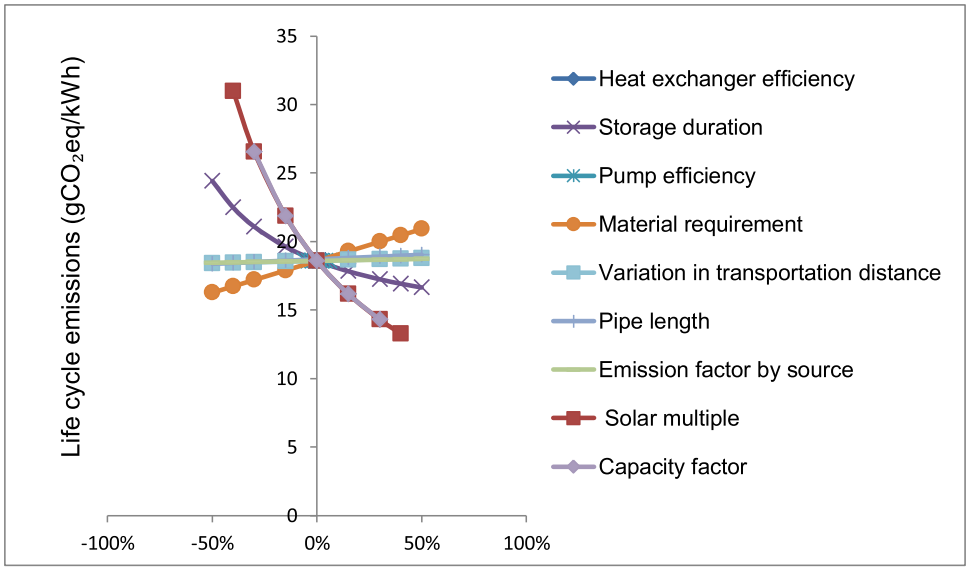

Fig. 10. GHG emissions sensitivity plot for thermochemical storage (S5).

Table 2
Base parameter values.

Base case values	S1[a]	S2–S5	Refs.
Heat exchanger efficiency (%)	95	95	[21]
Storage duration (hrs)	8.0	8.0	[45]
Generator efficiency (%)	95	95	[46]
Pump efficiency (%)	85	85	[34]
Solar multiple	1.75	1.75	[22]
Capacity factor (%)	40	40	[22]
Pipe length (m)	1700[b]	1400[c]	
Capacity (MW)	50	100	[26,27]
Electricity source emission factor (gCO_2-eq/kWh)	41	41	[47]

[a] S1, two-tank indirect sensible heat storage; S2, two-tank direct sensible heat storage; S3, one-tank direct sensible heat storage; S4, latent heat storage; S5, thermochemical storage.

[b] The pipe length was estimated using the plant layout of the Andasol solar power station.

[c] The pipe length was estimated using the plant layout of the Ivanpah solar power facility.

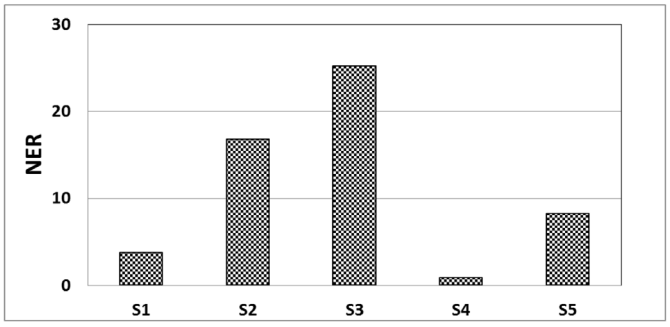

Fig. 11. NER for thermal energy storage technologies (S1: two-tank indirect sensible heat storage; S2: two-tank direct sensible heat storage; S3: one-tank direct sensible heat storage; S4: latent heat storage; S5: thermochemical storage).

production GHG emissions are a result of the operating conditions of ammonia. One of the factors affecting the operating conditions is the mass flow rate of ammonia, which requires high temperature and pressure and thus, the energy requirement and associated GHG emissions are high. Ammonia makes up nearly 70% of production GHG emissions. Concrete is another material that has important GHG emission contributions in S2–S5. This is because these systems have central towers in which heat from the sun is concentrated to heat the transfer medium (i.e., molten salt and ammonia). The central tower can be as high as 137 m, so a large amount of concrete is required to support the structure [27]. It is worth mentioning that the contribution of heat-tracing to the overall GHG emissions is minimal in cases S1–S4.

A sensitivity analysis was performed to determine which parameters are sensitive to the overall results. Figs. 9 and 10 shows the trends for S1 and S5. The other scenarios (S2–S4) follow the same trend as shown in the Supporting Information (Figures SI-1, SI-4, and SI-6). The capacity factor and the solar multiple are the most sensitive parameters. The capacity factor and the solar multiple are used to determine the amount of energy that can be generated from the CSP plant. The amount of energy stored in the system is the main function from which the functional unit is derived (kWh). A system with more storage capacity results in fewer GHG emissions per functional unit. Therefore, it would be ideal to increase energy production by increasing the solar multiple and the capacity factor, as they directly affect the energy produced from the system. For example, a solar multiple of one means the energy produced in the solar field equals the energy consumed by the turbine to generate electricity. A solar multiple of two, however, indicates that the solar field produces twice as much energy as what is required to generate electricity. The excess energy can be stored for later use during off-peak hours (i.e., night-time). In addition to the solar multiple, the capacity factor influences the energy produced. The capacity factor is the ratio of the actual energy to the theoretical energy produced per year [44]. In addition to the capacity factor and the solar multiple, the material requirement in S1–S4 and the storage duration in S5 are sensitive parameters, as shown in Figs. 9 and 10. In S5, heat is stored in a two-phase tank during an endothermic chemical reaction. This allows heat to be stored for long durations with minimal heat loss, thereby reducing associated GHG emissions [23].

3.2 Net energy ratio

The net energy ratio for TES systems was evaluated by considering the following key parameters: heat exchanger efficiency, storage duration, solar multiple, capacity factor, electricity source emission factor, generator efficiency, pump efficiency, pipe length, material requirement, and plant capacity. Table 2 lists the base case values for each parameter considered in the calculation. The capacity for S1 was assumed to be 50 MW, in keeping with capacity from an existing plant [26], while 100 MW was considered for S2–S5 since 133 MW is the

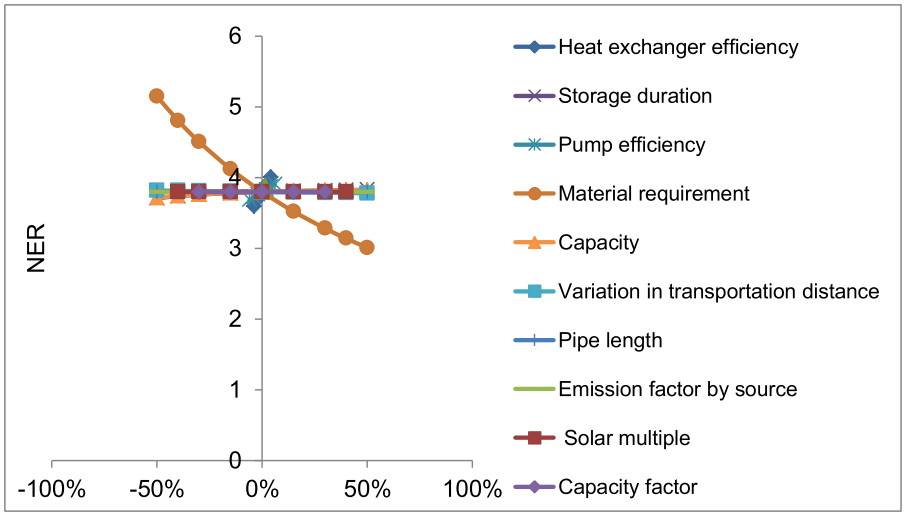

Fig. 12. NER sensitivity plot for 2-tank indirect sensible heat storage (S1).

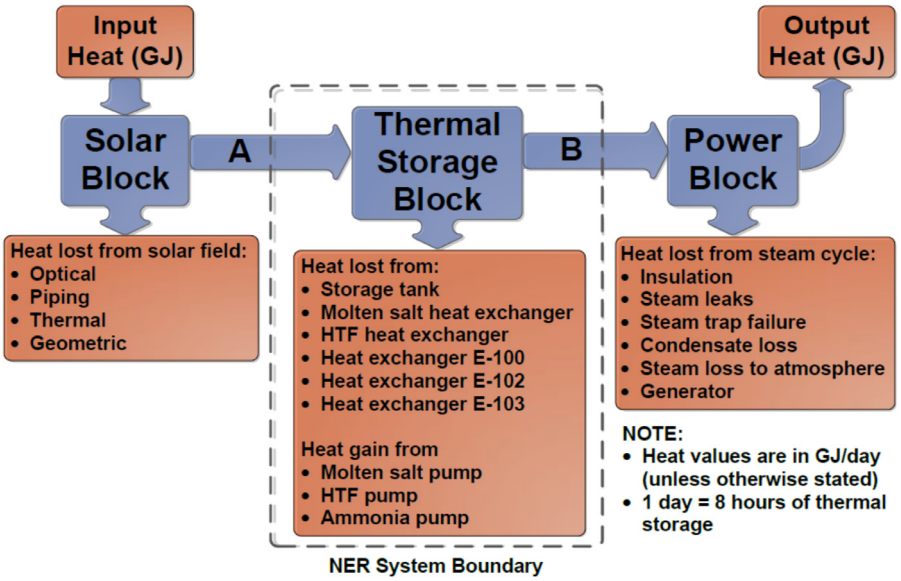

Fig. 13. NER block diagram for the thermal energy storage systems (S1: two-tank indirect sensible heat storage; S2: two-tank direct sensible heat storage; S3: one-tank direct sensible heat storage; S4: latent heat storage; S5: thermochemical storage).

largest turbine operating on a commercial scale in a CSP plant [27].

Fig. 11 shows the NER results for all five TES systems. S2 and S3 have higher NERs than the other systems. S2 and S3 lose less heat in the heat exchanger than S1. S1 requires additional heat exchanger to transfer heat from Dowtherm A©/Therminol VP© to the molten salt, which leads to heat loss. S2 and S3, on the other hand, use only one heat exchanger to generate superheated steam by exchanging heat between molten salt and water. S4 has the lowest NER of all the systems. This is mainly due to the high electricity requirement to produce the phase change material (lithium carbonate and potassium carbonate). The lower NER in S5 can be explained by the high energy demand to pump the ammonia at a high flow rate. S5 uses three heat exchangers, so there is heat loss, which affects the NER. The high energy demand to produce material such as stainless steel also contributes to S5's NER.

A sensitivity analysis was performed to determine which parameters have the largest impact on overall NER results. It can be seen in Fig. 12, heat exchanger efficiency, pump efficiency, and material requirement are highly sensitive parameters in S1. All other TES systems follow a similar trend as shown in the Supporting Information (Figures SI-2, SI-3, SI-5, and SI-7). The heat exchanger efficiency determines the amount of heat loss, which affects NER results. The pump efficiency is another parameter that has a high impact on NER values. Large quantities of heat transfer mediums such as molten salt, Dowtherm A©/Therminol VP©, and ammonia require high amounts of energy to be pumped from one heat exchanger to the next. The energy requirements to produce materials used in the construction of TES systems such as carbon steel, stainless steel, concrete, etc., are also key parameters influencing the NER value.

Fig. 13 and Table 3 show the heat loss and gain from individual equipment considered in the NER system boundary. The figure helps to visualize the energy flow in the system. The heat values for "A" and "B" in Table 3 refer to the heat delivered to and from the thermal storage block, respectively, as shown in Fig. 13.

3.3. Uncertainty analysis

There are different sources of uncertainty in LCA. They include input and output data, the emissions factor, modeling parameter uncertainties, and assumptions, to name a few. To capture the variability from these sources, an uncertainty analysis was conducted using a

Table 3
Heat values for the components in Fig. 13.

Thermal storage block	S1[a]	S2	S3	S4	S5
Input and output heat (GJ)					
Input heat	8555	18,174	18,074	18,078	18,587
A	3080	5089	5061	5062	5204
B	2172	4344	4344	4344	4344
Output heat	1440	2880	2880	2880	2880
Heat loss (GJ)					
Storage tank	102	58	19	7	N/A
Molten salt heat exchanger	424	719	719	719	N/A
HTF heat exchanger	446	N/A	N/A	N/A	N/A
Heat exchanger E-100	N/A	N/A	N/A	N/A	537
Heat exchanger E-102	N/A	N/A	N/A	N/A	748
Heat exchanger E-103	N/A	N/A	N/A	N/A	390
Heat gain (GJ)					
Molten salt pump	31	32	21	8	N/A
HTF pump	17	N/A	N/A	N/A	N/A
Pump 1	N/A	N/A	N/A	N/A	73
Pump 2	N/A	N/A	N/A	N/A	742
Heat loss from solar block (GJ)					
Optical	1968	5634	5603	5604	5762
Piping	855	1817	1807	1808	1859
Thermal	684	1454	1446	1446	1487
Geometric	1968	4180	4157	4158	4275
Heat loss from power block (GJ)					
Insulation	139	278	278	278	278
Steam leaks	163	326	326	326	326
Steam trap failure	78	156	156	156	156
Condensate loss	83	165	165	165	165
Steam loss to atmosphere	161	321	321	321	321
Generator	109	217	217	217	217

[a] S1, two-tank indirect sensible heat storage; S2, two-tank direct sensible heat storage; S3, one-tank direct sensible heat storage; S4, latent heat storage; S5, thermochemical storage.

Monte Carlo simulation. Figs. 14 and 15 show a box plot representation of the uncertainty ranges for NER and GHG emissions, respectively. Triangular distributions of the following parameters were considered for the analysis: plant capacity, storage duration, heat exchanger efficiency, pump efficiency, and generator efficiency. All other parameters considered in the analysis are listed in Table SI–8 in the Supporting Information. Each parameter has three input values: minimum, most likely, and maximum values. The most likely value is the base value, and minimum and maximum values were taken from the literature.

Except for S2 and S3, whose values overlap, there is clear variation in the overall NER values, as shown in Fig. 14. Though it is not clear whether S2 or S3 has the highest, both have higher NER values than the other three TES systems because they consume less energy during the production phase. Fig. 15 shows the GHG emissions' uncertainty results. The values overlap, which makes interpretation difficult. The overlap is largely a result of the GHG emissions from the production phase of manufacturing materials, which take the largest share of the global GHG emissions in all five TES systems. The high emissions in the production phase are due to the use of electricity and/or fossil fuels to run equipment in a manufacturing facility. The mean values shown by the white dot in Fig. 15 indicate that GHG emissions in S2 and S3 are lower than in the other systems; they are lower because less fossil fuel is consumed in S2 and S3 during the production phase.

4. Conclusions

The purpose of this study was to develop an Excel-based comparative model to evaluate life cycle GHG emissions and NER. Both GHG emissions and NER were used to compare the TES technologies in CSP applications (i.e., sensible heat, latent heat, and thermochemical storage). To make a reasonable comparison between each technology, a common system boundary was established by considering the material and energy requirements along with associated GHG emissions from resource extraction, material production, transportation, operation, dismantling, and disposal. With uncertainty considered, Fig. 15 shows an overlap in the results for each TES scenario. To compare the results for GHG emissions, the mean values (represented by the white dot) would have to be used. The mean GHG emission values for two-tank direct sensible heat storage and one-tank direct sensible heat storage are 15 gCO_2-eq/kWh, and 11 gCO_2-eq/kWh, respectively, which are lower than for the other systems. This is because the GHG emisions contributions from the production of the heat transfer medium in two-tank direct sensible heat storage and one-tank direct sensible heat storage are approximately 47% and 36% of the life cycle GHG emissions, respectively, below those of two-tank indirect sensible heat storage (63%) and latent heat storage (70%). Thermochemical storage, however, uses ammonia as the heat transfer medium. Since ammonia production is energy intensive, the GHG emissions from manufacturing ammonia are approximately 67% of the life cycle emissions. Thus, it would be ideal to consider the system that requires the least amount of material during the production phase as it will reduce GHG emissions considerably and improve the NER. For these reasons, two-tank direct sensible heat storage and one-tank direct sensible heat storage can be favourable when implemented commercially.

Acknowledgments

The authors thank the NSERC Energy Storage Technology(NEST) Network (RYERU NSERC 468468 Kumar) and the University of Alberta (UOFAB VPRGRF NEST KUMAR) for the financial support provided to carry out this research. We are also grateful to the NSERC/Cenovus/

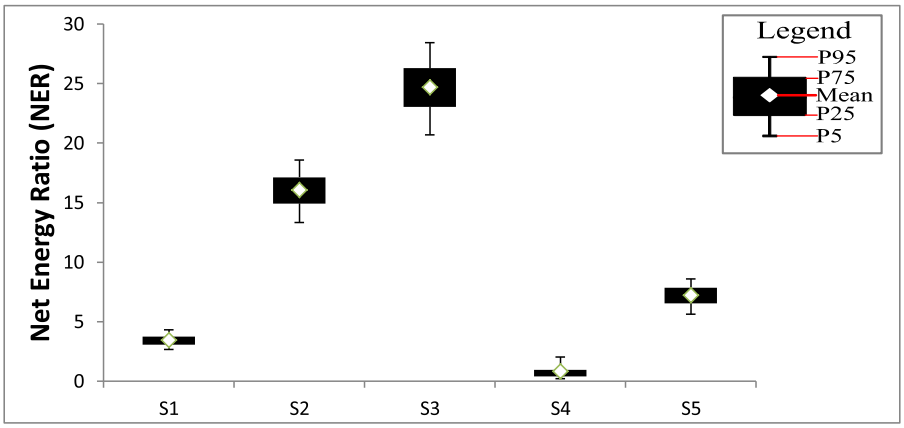

Fig. 14. NER uncertainty box plot for thermal energy storage systems (S1: two-tank indirect sensible heat storage; S2: two-tank direct sensible heat storage; S3: one-tank direct sensible heat storage; S4: latent heat storage; S5: thermochemical storage).

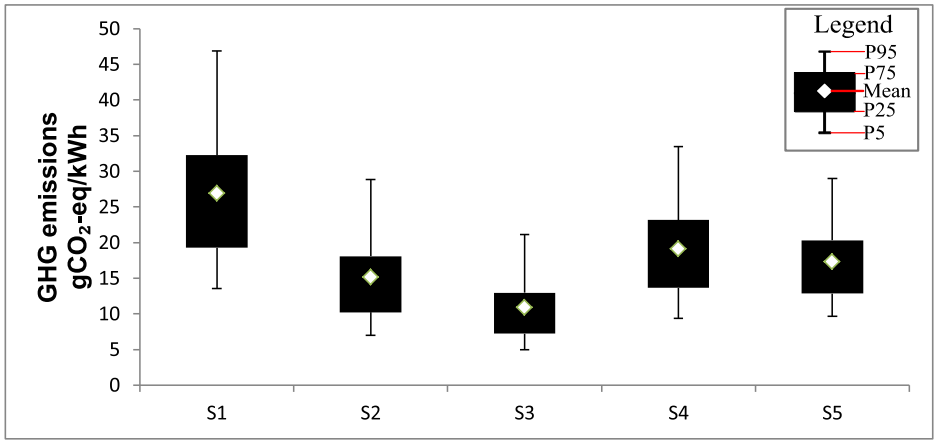

Fig. 15. Life cycle GHG emissions uncertainty box plot for thermal energy storage systems (S1: two-tank indirect sensible heat storage; S2: two-tank direct sensible heat storage; S3: one-tank direct sensible heat storage; S4: latent heat storage; S5: thermochemical storage).

Alberta Innovates Associate Industrial Research Chair in Energy and Environmental Systems Engineering and the Cenovus Energy Endowed Chair in Environmental Engineering for providing financial support for this project. The authors are thankful to Astrid Blodgett for editing this paper.

Supplementary material

Supplementary material associated with this article can be found, in the online version, at doi:10.1016/j.est.2019.100992.

References

[1] Intergovernmental panel on climate change, Climate Change 2014: Mitigation of Climate Change, vol. 3, Cambridge University Press, 2015.
[2] C. Philibert, Technology Roadmap: Solar Thermal Electricity—2014 Edition, International Energy Agency, Paris, France, 2014.
[3] E. Pihl, D. Kushnir, B. Sandén, F. Johnsson, Material constraints for concentrating solar thermal power, Energy 44 (2012) 944–954.
[4] D. Medveď, M. Kvakovský, V. Sklenárová, Latent heat storage systems, PhD thesis University of West Bohemia, 2010.
[5] J.J. Burkhardt III, G.A. Heath, C.S. Turchi, Life cycle assessment of a parabolic trough concentrating solar power plant and the impacts of key design alternatives, Environ. Sci. Technol. 45 (2011) 2457–2464.
[6] J.J. Burkhardt, G. Heath, E. Cohen, Life cycle greenhouse gas emissions of trough and tower concentrating solar power electricity generation, J. Ind. Ecol. 16 (2012) 93–109.
[7] N.A. Masruroh, B. Li, J. Klemeš, Life cycle analysis of a solar thermal system with thermochemical storage process, Renew. Energy 31 (2006) 537–548.
[8] E. Oró, A. Gil, A. De Gracia, D. Boer, L.F. Cabeza, Comparative life cycle assessment of thermal energy storage systems for solar power plants, Renew. Energy 44 (2012) 166–173.
[9] P. Denholm, Net Energy Balance and Greenhouse Gas Emissions from Renewable Energy Storage Systems, Energy Center of Wisconsin, 2003.
[10] R. Koppelaar, Solar-PV energy payback and net energy: meta-assessment of study quality, reproducibility, and results harmonization, Renew Sustain. Energy Rev. 72 (2017) 1241–1255.
[11] J.J. Burkhardt III, G. Heath, C. Turchi, Life cycle assessment of a model parabolic trough concentrating solar power plant with thermal energy storage, Proceedings of the ASME 2010 4th Internatinoal Conference on Energy Sustainabiality, Vol. 2 2010, pp. 599–608.
[12] J.T. Adeoye, Y.M. Amha, V.H. Poghosyan, Khachatur Torchyan, H.A. Arafat, Comparative LCA of two thermal energy storage systems for Shams1 concentrated solar power plant: molten salt vs. concrete, J. Clean Energy Technol. 2 (2014) 274–281.
[13] F. Magrassi, E. Rocco, S. Barberis, M. Gallo, A. Del Borghi, Hybrid solar power system versus photovoltaic plant: a comparative analysis through a life cycle approach, Renew. Energy 130 (2019) 290–304 2019/01/01/.
[14] C. Good, I. Andresen, A.G. Hestnes, Solar energy for net zero energy buildings–A comparison between solar thermal, PV and photovoltaic–thermal (PV/T) systems, Solar Energy 122 (2015) 986–996.
[15] Y. Lechón, C. de la Rúa, R. Sáez, Life cycle environmental impacts of electricity production by solarthermal power plants in Spain, J. Sol. Energy Eng. 130 (2008) 021012-021012-7.
[16] T. Larraín, R. Escobar, Net energy analysis for concentrated solar power plants in northern Chile, Renew. Energy 41 (2012) 123–133.
[17] International Organization for Standardization, ISO 14040 International Standard—Environmental Management—Life Cycle Assessment—Principles and Framework, Geneva, Switzerland, 2006.
[18] International Organization for Standardization ISO 14044 International Standard—Environmental Management—Life Cycle Assessment—Requirements and Guidelines, Geneva, Switzerland, 2006.
[19] I. Bhat, R. Prakash, LCA of renewable energy for electricity generation systems—a review, Renew. Sustain. Energy Rev. 13 (2009) 1067–1073.
[20] GREET® Model [Online]. Available:https://greet.es.anl.gov/.
[21] S. Thaker, A.O. Oni, A. Kumar, Techno-economic evaluation of solar-based thermal energy storage systems, Energy Conver. Manage. 153 (2017) 423–434.
[22] R.I. Dunn, P.J. Hearps, M.N. Wright, Molten-salt power towers: newly commercial concentrating solar storage, Proc. IEEE 100 (2012) 504–515.
[23] R. Dunn, K. Lovegrove, G. Burgess, A review of ammonia-based thermochemical energy storage for concentrating solar power, Proc. IEEE 100 (2012) 391–400.
[24] A. Luzzi, K. Lovegrove, E. Filippi, H. Fricker, M. Schmitz-goeb, M. Chandapillai, et al., Techno-economic analysis of a 10 MW e solar thermal power plant using ammonia-based thermochemical energy storage, Solar Energy 66 (1999) 91–101.
[25] PotashCorp.Available:http://www.potashcorp.com/contact/.
[26] Dow Canada-Prentiss. Available:http://www.dow.com/canada/prentiss/index.htm.
[27] MGX Minerals Inc. Available:https://www.mgxminerals.com/assets.html.
[28] (S&T)2 Consultants Inc., The Addition of Freight Emissions to GHGenius, prepared by Natural Resources Canada. https://ghgenius.ca/reports/GHGeniusFreightEmissions.pdf, 2010 (Accessed: 1 February 2018).
[29] S. Schlömer, T. Bruckner, L. Fulton, E. Hertwich, A. McKinnon, D. Perczyk, et al., Annex III: technology-specific cost and performance parameters, Climate Change (2014) 1329–1356.
[30] Infratech Corporation. Available:http://infratech.cc/contact/.
[31] ASME Boiler and Pressure Vessel Code, Section VIII Division 1, UG-126 Pressure Relief Valves to UG-129 Marking, ASME International, New York, 2010.
[32] Allowable Stress for Carbon Steel. Available:http://www.cis-inspector.com/asme-code-calculation-allowable-stresses.html.
[33] S.M.J. Miller. Designing Storage Tanks. Available:http://coade.typepad.com/files/ptq-q4-2016-designing-storage-tanks.pdf.
[34] E. McAllister, Pipeline Rules of Thumb Handbook: A Manual of Quick, Accurate Solutions to Everyday Pipeline Engineering Problems, Gulf Professional Publishing, 2013.
[35] ASME B31.3, Process Piping, American Society of Mechanical Engineering, 2002 http://pishgam.co.ir/files/8527/DomainTemplates/pishgam.co.ir/timages/ASME-B31.3.pdf . Accessed: 15 January 2017.
[36] M.B. Whitaker, G.A. Heath, J.J. Burkhardt III, C.S. Turchi, Life cycle assessment of a power tower concentrating solar plant and the impacts of key design alternatives, Environ. Sci. Technol. 47 (2013) 5896–5903.
[37] R. Moore, M. Vernon, C.K. Ho, N.P. Siegel, G.J. Kolb, Design Considerations for Concentrating Solar Power Tower Systems Employing Molten Salt, Sandia National Laboratories, Albuquerque, NM, 2010 SAND2010-6978.
[38] Thermon, Product Specifications MIQ™ Mineral Insulated Cable, (2019, June 21) Available: https://content.thermon.com/pdf/us_pdf_files/TEP0020-MIQ-Spec.pdf.
[39] Volume Flow and Temperature Rise in Pump. Available:http://www.engineeringtoolbox.com/pumps-temperature-increase-d_313.html.
[40] Airec Heat Exchangers. Available:http://airec.se/heat-exchangers/.
[41] Molten Salt Energy Storage. Available:http://www.solarreserve.com/en/technology/molten-salt-energy-storage.
[42] S. Kuravi, Y. Goswami, E.K. Stefanakos, M. Ram, C. Jotshi, S. Pendyala, et al., Thermal energy storage for concentrating solar power plants, Technol. Innov. 14 (2012) 81–91.
[43] A. Modi, C.D. Perez-Segarra, Thermocline thermal storage systems for concentrated solar power plants: one-dimensional numerical model and comparative analysis, Solar Energy 100 (2014) 84–93.

[44] S. Izquierdo, C. Montanes, C. Dopazo, N. Fueyo, Analysis of csp plants for the definition of energy policies: the influence on electricity cost of solar multiples, capacity factors and energy storage, Energy Policy 38 (2010) 6215–6221.
[45] Concentrating Solar Power, ed: IRENA, 2012.
[46] A.G. McDonald, H. Magande, Introduction to Thermo-Fluids Systems Design, John Wiley & Sons, 2012.
[47] Intrinsik Corporation. Greenhouse Gas Emissions Associated with Various Methods of Power Generation in Ontario. https://www.opg.com/darlington-refurbishment/Documents/IntrinsikReport_GHG_OntarioPower.pdf, 2016 (Accessed: 24 May 2018).